Desalination and Water Treatment
www.deswater.com

doi: 10.1080/19443994.2013.839397

53 (2015) 475–484
January

Taylor & Francis
Taylor & Francis Group

Adsorption of di-butyl phosphate on activated alumina: equilibrium and kinetics

N.K. Pandey*, P. Velavendan, U. Kamachi Mudali, R. Natarajan

Reprocessing Group, Indira Gandhi Centre for Atomic Research, Kalpakkam, Tamilnadu 603102, India
Tel. +91 4427480126; Fax: +9144 27480126; email: nkpandey@igcar.gov.in

Received 5 March 2013; Accepted 20 August 2013

ABSTRACT

The rate of removal of di-*n*-butyl phosphate (DBP) by sorption on activated alumina (AA) has been studied in batch conditions. The rate of adsorption of DBP is initially rapid for about 10–20 min and reaches a maximum in about two hours. The Langmuir and Freundlich isotherm equations have been used to describe the partitioning behavior of the system. Kinetic modeling analysis of the pseudo-first-order, pseudo-second-order, and pore diffusion model, coupled with the observed Langmuir or Freundlich isotherm equations showed that pseudo-second-order equation and pore diffusion model to be the most appropriate models for the description of transport of DBP within AA particles. The agreement between the model predictions and experimental data indicated that adsorption and diffusion of DBP can be simulated by the proposed models. From analysis of the experimental kinetic data, effective diffusivity has also been estimated and is found to be in the range of 10^{-9} cm^2/s.

Keywords: Adsorption kinetics; Solvent regeneration; Adsorbent; Activated alumina

1. Introduction

To recover uranium and plutonium from spent nuclear fuel, tri-butyl phosphate (TBP) diluted with *n*-dodecane (NDD) or a hydrocarbon diluent is widely used as a solvent in the plutonium uranium reduction extraction (PUREX) process of nuclear fuel reprocessing plant [1]. The process aims at nearly complete recovery of uranium and plutonium from fission products in the spent fuel discharged from the reactor. It is widely recognized that the TBP and hydrocarbon diluents are degraded due to hydrolytic and radiolytic reactions, forming activity-binding degradation products that can cause product losses, poor separation efficiencies, and emulsions which could interfere with process operations [2–5]. The primary degradation products (i.e. dibutyl phosphate, monobutyl phosphate, phosphoric acid, and butanol) are produced from the hydrolytic and dealkylation reactions of the TBP when contacted with nitric acid at relatively high temperatures. The secondary degradation products (nitroparraffins, aldehydes, ketons, and carboxylic acids), on the other hand are originated from the radiolytic reactions of diluents when exposed to intensive radiation [6–12]. Hence, the solvent needs to be purified before it is recycled back to process. In the PUREX process, the spent solvent is continuously regenerated by scrubbing with sodium carbonate/hydroxide and phosphoric acid solutions after each pass through the process and most of the radioactivity belonging to primary degradation products is removed [13,14]. Residual activity due to

*Corresponding author.

secondary degradation products, however, cannot be removed by these washing solutions as these long-chain soluble organic compounds tend to remain in the solvent even after scrubbing with carbonate washing solutions to again complex fission products when the solvent is recycled [13,14]. Thus, other methods such as vacuum distillation [15–17], steam stripping, and flash distillation [18–20] have been reported to be effective techniques, but they are limited by the maximum allowable distillation temperature that could lead to significant decomposition of the TBP tar residues. Several investigators have studied an adsorption-based solvent cleanup process to improve recycle solvent performance [21–26]. These studies have shown that solid adsorbents such as activated alumina (AA) and base-treated silica gel have the potential for removal of some of the activity-binding degradation products.

Adsorption is one of the most reliable and versatile physical treatment, whose effectiveness and economic sustainability is related to the type of sorbent. AA is widely used adsorbent for many applications because of the chemical properties of its surface. It is highly porous in nature and has high surface area (150–350 m^2/g). Alumina, owing to its amphoteric properties (acting either as a base, acid, or neutral pH) provides chromatographers an able adsorbent to separate a multitude of compounds, surpassing the results achievable with silica gels. This means alumina can act as a weak ion exchanger exhibiting anionic or cationic properties, in addition to acting as an adsorbent.

An understanding of the adsorption kinetics of di-*n*-butyl phosphate (DBP) within AA particles will insure a better prediction of the transport behavior of DBP in columns. No information related to the description of both adsorption equilibrium and kinetics of DBP within AA particle is available in the literature.

In the present study, fundamental aspects of adsorption equilibrium and kinetics of DBP on AA have been investigated to show the mechanistic aspect of the process. Sorption data have been correlated with the Langmuir and Freundlich isotherm models. Experiments were conducted to determine the adsorption kinetics for di-butyl phosphate and pseudo-first-order, pseudo-second-order, and pore diffusion model have been used to interpret the observed experimental adsorption kinetic data. Based on the results, pore diffusion coefficient and intraparticle effective diffusivity of DBP in AA have been estimated.

2. Transport mechanism of solute in sorbent (Batch kinetic studies)

Adsorption is a surface phenomenon, but it also involves the transfer of solute from one phase to another. Various adsorption kinetic models have been adopted to describe the behavior of batch sorption process under different experimental conditions [10–11]. Sorption kinetics are however controlled by the following steps: (1) external mass transfer of solute from bulk solution to the outer surface of particles (film diffusion), (2) diffusion of solute from the sorbent surface to the pores of the particles, and (3) the adsorption of solute on the active sites of the pore surface. Fig. 1 shows the schematic representation of solute transfer into the adsorbent phase.

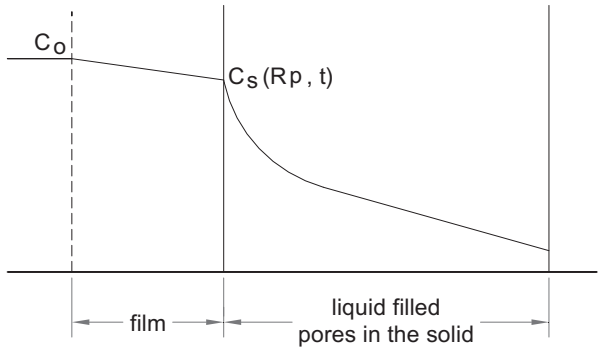

Fig. 1. Schematic representation of solute into the adsorbent phase.

A nonlinear concentration profile is expected within the sorbent phase because adsorption and diffusion occur simultaneously inside the particle. Contribution of intraparticle diffusion mechanism can be tested by applying the Webber and Morries equation [27]. According to intraparticle diffusion mechanism, the plot of the amount adsorbed (q) versus square root of time should be linear. If intraparticle diffusion is involved in the adsorption process, then the plot of square root of time versus the uptake would result in a linear relationship passing through origin, and the intraparticle diffusion would be the controlling step. If the plot does not pass through the origin, then this is indicative of some degree of boundary layer control. Further, it shows that the intraparticle diffusion is not the only controlling step and there may be other processes that may control the rate of adsorption. If the plots are not totally linear and not passing through origin, then intraparticle diffusion could not be the only mechanism involved.

2.1. Mathematical model for the transport of solute from the solution into adsorbent phase

Development of model equations is based on the following assumptions: (1) diffusivity is constant at constant temperature and pressure, (2) AA grains are considered as spherical and porous, (3) the adsorption

sites are uniformly distributed throughout the grains, and (4) the external mass transfer coefficient and diffusivity are constant for the range of solute concentrations under consideration.

The rate of DBP concentration change in the bulk solution is proportional to the concentration difference between the bulk phase and the outer surface of the particle. The mass balance in the bulk liquid phase describes the relation between the decreasing solute concentration in solution phase and mass transfer into the solid phase and can be written as [28]:

$$-\frac{\partial C}{\partial t} = \frac{3M_p k_f}{VR\rho_p}(C - C_s) \tag{1}$$

where C is the bulk concentration of solute in the solution phase, and C_s is the concentration of solute at the outer surface of the spherical particle. R represents the radius of the particle, ρ_p is the density of powder, M_p is the total mass of the particle, V is the volume of solution used in the batch reactor, and k_f is the external mass-transfer coefficient. Here, mass flow rate of solute through external film is proportional to the concentration difference between bulk phase DBP concentration (C) and DBP concentration at the particle surface C_s (R_p, t).

The mass balance of DBP within a spherical particle at a distance r from the center of particle is given as (from Fick's 2nd Law of diffusion in spherical co-ordinate):

$$\varepsilon_p \frac{\partial C_r}{\partial t} + \rho_p \frac{\partial q_r}{\partial t} = D_e \frac{1}{r^2}\frac{\partial}{\partial r}\left(r^2 \frac{\partial C_r}{\partial r}\right) \tag{2}$$

where D_e is the effective diffusivity of solute within the particle (could be treated as a combination of pore diffusion and surface diffusion), ε_p is the porosity, C_r is the solution concentration of DBP within the pores of alumina particle, and q_r is the solid phase concentration of DBP. The first and second terms on the left hand side of Eq. (2) give accumulation of DBP in the void space of the adsorbent particles and solid phase, respectively.

The Langmuir isotherm $\left(q_r = \frac{q_m K_L C_r}{1+K_L C_r}\right)$ can be used for the correlating of C_r and q_r. Then Eq. (2) becomes

$$\frac{\partial C_r}{\partial t} = \frac{D_e}{\varepsilon_p + (\rho_p K_L q_m)/(1 + K_L C_r)^2}\frac{1}{r^2}\frac{\partial}{\partial r}\left(r^2 \frac{\partial C_r}{\partial r}\right) \tag{3}$$

The initial and boundary conditions can be written as:

$$t = 0 : C = C_0,\ Cr = 0 \tag{4}$$

$$r = 0 : \left(\frac{\partial C_r}{\partial r}\right)_{r=0} = 0 \tag{5}$$

$$r = R : k_f(C - C_S) = D_e\left(\frac{\partial C_r}{\partial r}\right)_{r=R} \tag{6}$$

Eqs. (1–6) are solved numerically by converting them into dimensionless coupled-ordinary differential equations by finite difference methods in order to obtain concentration profiles in the particle (solution procedure is described in Appendix A).

2.2. Other kinetic models

2.2.1. Pseudo-first-order kinetic model

Lagergren's equation [29] was the first kinetic equation used extensively to describe the sorption kinetics of sorption of liquid/solid system. This model assumes that the rate of change of solute uptake is directly proportional to the difference in saturation concentration and the amount of solid uptake with time. Lagergren's first-order rate equation is called pseudo-first-order equation and the equation is

$$\frac{dq}{dt} = k_1(q_e - q) \tag{7}$$

where q and q_e in mol/g are the amount adsorbed at time t and at equilibrium, respectively, and k_1 is the pseudo-first-order rate constant, (min^{-1}) for the adsorption. After integration and applying boundary conditions at $t = 0$: $q = 0$, and at $t = t$: $q = q$ the integrated form of Eq. (7) becomes

$$\ln(q_e - q) = \ln q_e - k_1 t \tag{8}$$

The plot of $\ln(q_e - q)$ vs. t gives a straight line for first-order kinetics, which allows computation of the adsorption rate constant, k_1.

2.2.2. Pseudo-second-order kinetic model

A pseudo-second-order model [30] also describes the sorption kinetics. The differential equation for the pseudo-second-order kinetic model is given by:

$$\frac{dq}{dt} = k_2(q_e - q)^2 \tag{9}$$

where k_2 is the equilibrium rate constant of pseudo-second-order sorption and its unit is (g/mg min). The observed second-order rate constant k_2 is also

expected to be dependent on the pore diffusion parameters, initial adsorbate concentration, and the amount of adsorbent charged to the adsorber. Integrating Eq. (9) for the boundary conditions $t = 0$ to $t = t$ and $q = 0$ to $q = q$ gives:

$$\frac{t}{q} = \frac{1}{k_2 q_e^2} + \frac{1}{q_e} t \tag{10}$$

If pseudo-second-order kinetics is applicable, the plot of t/q vs. t gives a linear relationship, which allows computation of k_2 and q_e from the intercept and slope of the plot.

3. Experimental

3.1. Adsorption isotherm measurements

All chemicals and reagents used were of analytical grade. The characteristics of AA are reported in Table 1.

For the measurement of adsorption isotherm, a known volume (V) of the organic (30 vol. % TBP) having DBP concentration of C_0 was placed in a well-stirred vessel. A weighed amount of AA was added to it. The content of the vessel was mixed for about one hour and then allowed to settle for about four hours by which time the solution concentration reached an equilibrium value. The solution was then sampled, centrifuged, and analyzed for DBP concentration by Ion Chromatography. The experiment was repeated by taking different volumes of solution having same concentration or different amount of adsorbent.

3.2. Adsorption rate measurement

The influence of contact time of DBP onto the surface of alumina particle was studied in a separate experiment by measuring the change in the concentration of DBP in solution with time. Liquid samples were withdrawn at regular intervals and analyzed for DBP concentration until an equilibrium value was attained. Samples were drawn more frequently in the initial phase of the experiment than towards the end, to achieve suitable distribution of the measured concentration. Sample size was 1 mL at higher concentration and up to 2 mL at lower concentration. About eight samples were taken but the system was treated as being at constant volume in evaluating the results.

Table 1
Characteristics of activated alumina

Adsorbent	Activated alumina from E-Merck
Surface area (BET)	~155 m^2/g
Avg. particle size	~150 mesh
Pore diameter	58 Å
Porosity	~28%
Bulk density	1.056 g/cm^3
Fe_2O_3	0.02 (% max)
SiO_2	0.02 (% max)

3.3. Analytical method

Quantitative analysis of DBP in the solution was done by using Metrohm-make modular Ion Chromatograph equipped with 819 IC detectors, 820 IC separation center, 818 IC pump (Isocratic), 833 IC liquid handling unit, and 830 IC interface. The sample was injected through a 20 µl PEEK (Polyetheretherketone) loop fitted with the injector. IC net 2.3 Metrohm software was used for instrument control and data acquisition. Metrosep A Supp 5–250, 250 mm(L) × 4 mm(ID) with Guard column Metrosep A Supp 4/5 was used for separation. About 3.2 mM Na_2CO_3 + 1.0 mM $NaHCO_3$ with a flow rate of 0.7 mL/min was used as eluent.

To determine DBP in the organic solution, the sample was treated with 1% sodium carbonate and sodium hydroxide mixture; the contents were mixed well and allowed to settle and a known aliquot of the aqueous phase was then taken in a 100 mL standard flask and made up to the mark with high purity water. The aqueous phase was injected through 20 µl PEEK loop and subsequent ion-exchange separation in anionic column followed by suppressed conductivity detection chromatograms were obtained. The peak area thus obtained for the samples were compared with that of the standard for the estimation of DBP concentration in organic phase.

4. Results and discussion

4.1. Adsorption isotherm

Equilibrium data are commonly reported in the form of an isotherm, which is a diagram showing the variation of the equilibrium adsorbent phase concentration with the fluid phase concentration at a fixed temperature. The equilibrium amount of DBP on AA is determined from the difference between feed concentration and equilibrium concentration and is given by [31]:

$$q_e = \frac{V(C_o - C_e)}{M_P} \tag{11}$$

where M_p is the mass of adsorbent used. A series of experimental points for the adsorption of DBP on AA are plotted to give the adsorption isotherm (i.e. amount of DBP adsorbed per unit mass of alumina at equilibrium versus the final concentration of the respective solution) which is depicted in Fig. 2. The isotherms are regular, positive, and concave to the solution phase concentration axis. The initial rapid adsorption gives way to a slow approach to equilibrium at higher adsorbate concentration. Two commonly used mathematical expressions to describe adsorption equilibria namely: Langmuir and the Freundlich isotherm models were tested with experimental data.

4.1.1. Langmuir model

The Langmuir model [32] is a theoretical approach that was originally applied to gas adsorption on to solids but can also be used for adsorption from solutions. This model assumes that every part of the adsorbent surface has the same energy of adsorption, adsorption at local sites without interactions between adsorbate molecules and the amount adsorbed is confined to monolayer. The Langmuir model is expressed as:

$$\frac{q_e}{q_m} = \frac{K_L C}{1 + K_L C} \tag{12}$$

where K_L is the Langmuir isotherm constant and q_m is the capacity of the adsorbent for mono-layer coverage and these are evaluated through linearization of Eq. (12).

$$\frac{1}{q_e} = \frac{1}{q_m} + \frac{1}{q_m K_L C} \tag{13}$$

The slope and intercept of the plot $(1/q_e)$ vs $(1/C)$ give the value of K_L and q_m which were found to be $3.4364 \times 10^6\,\mathrm{cm^3/mol}$ and $3.8545 \times 10^{-4}\,\mathrm{mol/g}$, respectively.

4.1.2. Freundlich model

Eq. (14) is attributed to Freundlich [33], is an empirical and nonlinear in concentration (pressure) and is generally used for liquid system:

$$q_e = K_F C^{1/n} \tag{14}$$

where K_F and n are constants and logarithmic linearization of Eq. (14) facilitates the determination of model constants K_F and n. The numerical values of these constants for the present work are 0.0015 and 4.1455, respectively. The Langmuir model of isotherm fits the experimental data better than Fruendlich model as is observed from Fig. 2.

4.2. Comparison of experimental and the model predicted results

The time dependence of the rate of adsorption of TBP on AA at different feed concentrations was obtained by batch contact-time experiments. Fig. 3 shows the results of contact time experiments. It is observed that the equilibrium time is independent of initial concentration of adsorbate in solution and is established in about two hours.

The model Eqs. (1) and (3) describing the transport of DBP from solution phase to AA particles was solved numerically by the fourth-order Runge–Kutta method using ODE-45 solver of MATLAB software.

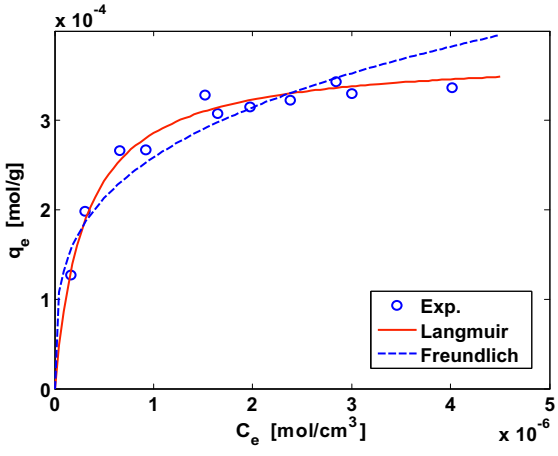

Fig. 2. Equilibrium data of DBP on activated alumina.

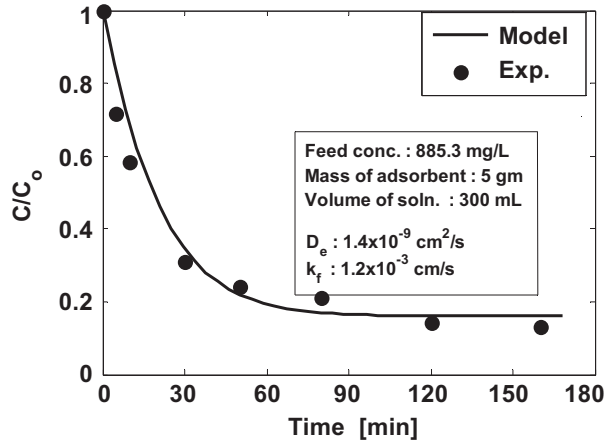

Fig. 3. Comparison of experimental data and simulation results for DBP adsorption on activated alumina.

The agreement between the experimental results and the model predicted values (as illustrated in Fig. 3) is found to be good. The external mass transfer (k_f) and the effective diffusivity (D_e) are the two unknown parameters which are estimated by superimposing the experimental data on to the diagrams of numerical solution of model equations (Fig. 3). The following algorithm was employed to find D_e and k_f: at the first step the value $k_f = k_f^{(0)}$ was fixed and D_e value was varied to obtain the best fit of the results of numerical solution of Eqs. (7) and (8) to the experimental curves for batch adsorption and $D_e^{(1)}$ was determined. Subsequently, $D_e = D_e^{(1)}$ was fixed and the value of k_f was varied to obtain the best fit again to the experimental curves to obtain $k_f^{(1)}$. In the second step, $k_f = k_f^{(1)}$ was fixed in the same way to define $D_e^{(2)}$ and $k_f^{(2)}$. This step was repeated until an acceptable accuracy is attained to get the optimal D_e and k_f values. The value of effective diffusivity (D_e) was found to be $1.4 \times 10^{-9}\,\mathrm{cm^2/s}$.

Sensitivity analysis for the changes of k_f and D_e was performed. Fig. 4 represents the effect of k_f on model prediction results. If k_f is 10–100 times smaller than the estimated value $1.2 \times 10^{-3}\,\mathrm{cm/s}$, then the initial removal rate of DBP is slower. However, when k_f value exceeds the estimated value, the removal rate remained unchanged. Because the external mass transfer is sufficiently fast for DBP removal, the increase in the external mass transfer coefficient has no influence on the entire removal process.

Fig. 5 shows the effect of diffusivity. If D_e value is 10–100 times higher than the specified value ($1.4 \times 10^{-7}\,\mathrm{cm^2/s}$), then the removal rate becomes faster. However, when D_e is smaller than the estimated value, the removal rate is almost similar to that of estimated value. Thus, from simulation it was observed that effect of D_e on removal rate is less sensitive in comparison to the external mass transfer coefficient.

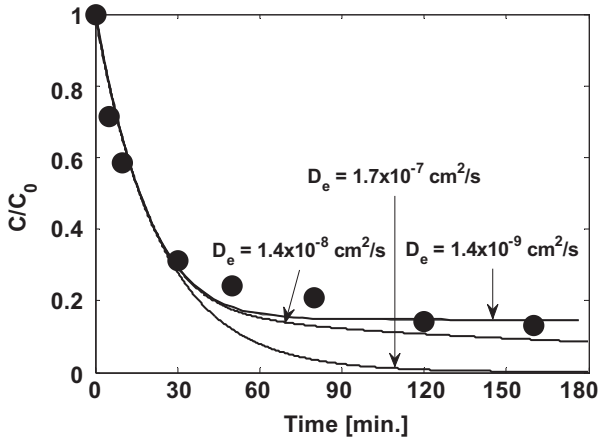

Fig. 5. Effect of effective diffusivity on model prediction.

A comparison between the experimental and calculated values using pseudo-first and second-order kinetic model for the amount of DBP adsorbed on AA with time is made in Fig. 6. A good agreement between experimental and prediction data based on pseudo-second-order model was noticed, while pseudo-first-order kinetic model does not fit the experimental data.

Fig. 7 shows the curve fitting plots of pseudo-second-order model for the estimation of rate constant, k_2 of the model and equilibrium concentration (q_e) of solute in adsorbent phase.

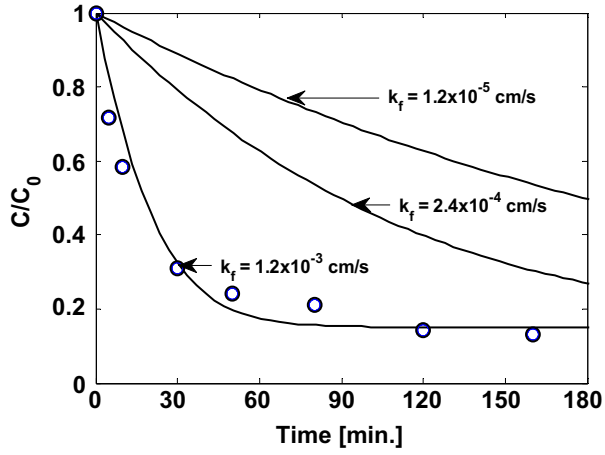

Fig. 4. Effect of external mass transfer coefficient on model prediction.

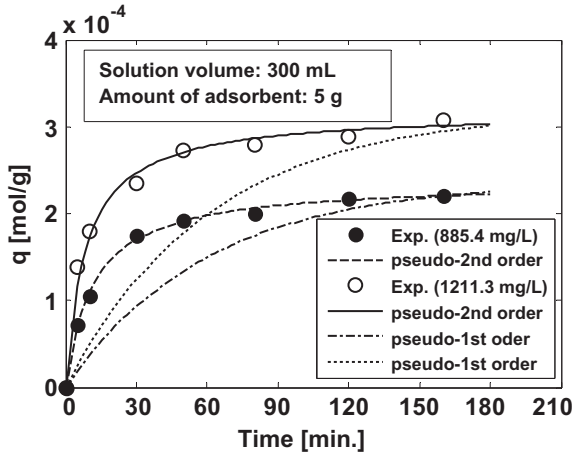

Fig. 6. Comparison between experimental and calculated values using pseudo-first-order and pseudo-second-order kinetic model of amount of DBP adsorbed on activated alumina with time.

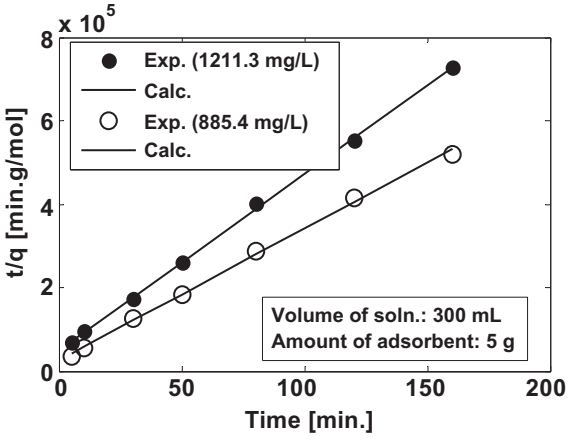

Fig. 7. Plot of t vs. t/q for the estimation of k_2 and q_e.

The values of k_2 and q_e obtained for different initial concentration of DBP in organic phase using this model are presented in Table 2. From Table 2, it is observed that the rate constant k_2 is nearly independent of initial adsorbate concentration in the feed solution.

4.3. Another simplified method for effective diffusivity

For the measurement of the diffusion coefficient in solid, one of the several commonly used methods involves recording the concentration history of the solution during transport of solute from a constant volume of solution onto adsorbent particles. On the other hand, solution of the diffusion equation with appropriate boundary conditions provides a theoretical expression for the fractional uptake of solute in terms of the variable $D_e t$. Comparison of experimental curve with the theoretical one, gives diffusion coefficient.

For batch adsorption of solute on spherical particles, it has been reported that for $(q/q_e) < 0.3$ and for a system with constant diffusion coefficient, the solution of diffusion equation based on Fick's second law can be approximated as [31,34]:

$$\frac{q(t)}{q_e} = \frac{6}{R}\left(\frac{D_e t}{\pi}\right)^{0.5} \quad (15)$$

or

$$q(t) = \frac{6q_e}{R}\left(\frac{D_e t}{\pi}\right)^{0.5} \quad (16)$$

In general, mechanism of the adsorption process can be determined by plotting the amount adsorbed (q) against square root of time ($t^{1/2}$) [35]. It is noticed in Fig. 8 that the plot of amount adsorbed vs $t^{1/2}$ can be classified into three portions. Two linear and one curved portion and the transition depend on adsorbate concentration and type of adsorbent. The first linear portion signifies instantaneous adsorption stage. The spherical particles of adsorbent are considered to be surrounded by a boundary layer of fluid film through which solute must diffuse prior to external adsorption on the adsorbent surface. This step is responsible for the first section. The second portion of the plot represents intraparticle diffusion step and the third linear portion is the final equilibrium stage. In this step, the concentration of solute on the adsorbent surface starts to decrease which results in the decrease of diffusion rate.

In the batch mode process where sufficient turbulence is provided by means of high degree of agitation, pore diffusion in addition to surface adsorption is often the rate-limiting step. In the present investigation, since, sufficient mixing of organic solution containing DBP and porous alumina powder was provided, it is likely that pore diffusion is the rate limiting step. The slope of the intermediate linear portion of the plot, $t^{1/2}$ *vs*. q provides intraparticle effective diffusion coefficient as per the Eq. (16).

The values of D_e calculated using numerical simulation are listed in Table 3 along with those calculated using Eq. (15). A marginal variation is observed in the values of effective diffusion coefficient calculated using the two different methods.

It is to be noted that relation given by Eq. (15) is an approximation, which is valid over a small range of time and for a system of constant diffusion coefficient. Often the diffusion coefficient of dilute solutions can be assumed as constant for practical purposes and this relation can be used for the estimation of intraparticle effective diffusion coefficient. The time

Table 2
Kinetic parameters for the adsorption of DBP on activated alumina

S. no.	Feed concentration (mol/L)	Adsorbent mass (g)	k_2 (g mol^{-1} min^{-1})	q_e (mol/g)
1	1211.2 mg/L	5	355.973	3.173E-04
2	885.3 mg/L	5	364.768	2.363E-04

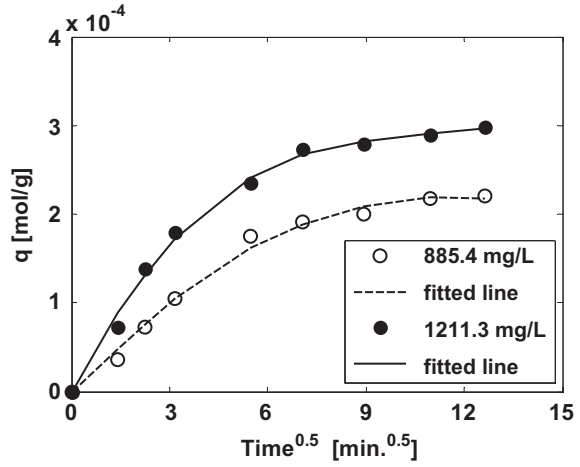

Fig. 8. Amount of DBP adsorbed on activated alumina from organic at two different concentrations against square root of time.

Table 3
Values of diffusion coefficient calculated from numerical simulation and using Eq. (15)

C_o (mg/L)	D_e (cm^2/s)
885.3 mg/L	1.4×10^{-9} [numerical simulation]
885.3	3.2×10^{-9} [Eq. (15)]
1211.4	5.4×10^{-9} [Eq. (15)]

period over which the diffusion coefficient (D_e) was calculated using Eq. (15) varied approximately between two to three minutes.

5. Conclusion

Equilibrium and kinetics of sorption of DBP on AA for the removal from organic solvent (30 vol.% TBP in NDD) have been carried out experimentally. Theoretical models were evolved to explain experimental data. Following conclusions could be drawn from the results of the present investigation:

(1) The adsorption isotherm has been correlated using Langmuir and Freundlich model of adsorption. The Langmuir isotherm fits well with experimental data.
(2) The mechanism of adsorption involves an initial rapid rate for the removal of DBP due to surface diffusion followed by intrapaticle diffusion. At later stages, rate of adsorption of DBP decreases with time. This is possibly due to the decreased concentration gradient.
(3) The diffusion model was numerically assessed and there was conformity between theoretical prediction and batch experimental data. Furthermore, theoretical values of D_e and k_f were estimated from diffusion model.
(4) Kinetic modeling analysis of the pseudo-first-order, pseudo-second-order, and pore diffusion model, coupled with the observed Langmuir or Freundlich isotherm equations showed that the pseudo-second-order equation and pore diffusion model have been found to be most appropriate models for the description of transport of DBP within AA particles.

Acknowledgments

The authors wish to express their sincere thanks to Mrs. Gyanasoundary and Mr. Suresh Borado for their assistance in the experimental works. The authors also wish to express their gratitude to Dr. PR. Vasudeva Rao, Director, IGCAR for his constant encouragement and guidance during the course of this investigation.

Nomenclature

C — bulk solution concentration of DBP at any time t, (mol/cm^3)
C_e — equilibrium concentration of DBP (mol/cm^3)
C_i — interfacial concentration of DBP (mol/cm^3)
C_0 — initial concentration of DBP in solution (mol/cm^3)
C_r — pore liquid concentration of DBP at any time t (mol/cm^3)
C_s — concentration of DBP at the particle surface (mol/cm^3)
D_e — effective diffusivity (cm^2/s)
k_1 — pseudo-first-order rate constant for the adsorption (min^{-1})
k_2 — pseudo-second-order sorption (g/mg min)
k_f — external mass transfer coefficient (cm/s)
K_F — Freundlich constant (mol$^{(n-1)/n}$.cm$^{(3/n)}$/g)
K_L — Langmuir isotherm constant (cm^3/mol)
M_p — mass of the particle (g)
n — Freundlich constant
q — amount adsorbed at time t (mol/g)
q_e — amount adsorbed at equilibrium (mol/g)
q_m — maximum adsorption capacity on solid phase for monolayer formation (mol/g)
q_r — solid phase concentration of DBP at any time t (mol/cm^3)
r — radial distance from the center of the particle (cm)
R — radius of the particle (cm)
V — volume of the solution (mL)
t — time (s)
ρ_p — density of the particle (g/cm^3)
ε_p — porosity of the particle

References

[1] C. Misikas, W. Schulz, J.O. Liljenzin, Solvent extraction in nuclear science and technology, In: J. Rydberg, M. Cox, C. Musika, G. Chopin (Eds.), Solvent Extraction Principles and Practice, second ed., Markel Dekker, New York, NY, pp. 507–557, 2004.

[2] Z. Nowak, M. Nowak, J. Michalik, A. Owczarczyk, ESR study of irradiated TBP–dodecane–HNO_3 system, Radiochem. Radioanal. Lett. 12 (1972) 2–3.

[3] C.A. Blake Jr., Solvent Stability in Nuclear Fuel Reprocessing-evaluation of the Literature, Calculation of Radiation Dose and Effects of Iodine and Ilutonium, Oak Ridge National Laboratory, ORNL—4212, 1968.

[4] Z. Nowak, Radiative and thermal variations on the dodecane—30% TBP–HNO_3 system, Nukleonika 18 (1973) 447–454.

[5] S.C. Tripathi, A. Ramanujam, K.K. Gupta, P. Bindu, Studies on the identification of harmful radiolytic products of 30% TBP–dodecane–HNO_3 by gas-chromatography. II. Formation of high molecular weight organophosphates, Sep. Sci. Technol. 36 (2001) 2863–2883.

[6] L.L. Burger, The chemistry of tributyl phosphate: A review, USAEC Rep. HW-40920, Hanford Works (1955).

[7] W. Davis, Jr., Radiolytic behavior, in: W.W. Schulz, J. Navratil (Eds.), Science and Technology of Tri-butyl Phosphate, Vol. 1, CRC Press, FL, 1984 (Chapter 7), pp. 221–226.

[8] M. Benedict, H. Pigford, H.W. Levi, Nuclear Chemical Engineering, McGraw-Hill, New York, NY, 1981.

[9] J.C. Neace, Diluent degradation products in the PUREX solvent, Sep. Sci. Technol. 18(14–15) (1983) 1581–1594.

[10] L. Stieglitz, Investigation on the Nature of Degradation Products in the System 20 Volume Percent Tributyl Phosphate - dodecane - nitric Acid. I - Enrichment of Complexing Products and Infra-red Studies, Paper 131, International Solvent Extraction Conference, London, 1971.

[11] R. Becker, L. Stieglitz, Investigation of Degradation Products of the System Tributyl Phosphate - dodecane - nitric Acid. II - Analysis of Products, KFK-1373, November 1973.

[12] C.A. Blake, W. Davis, Jr., J.M. Schmitt, Properties of degraded TBP-AMSCO solutions and alternative extraction diluent systems, Nucl. Sci. Eng. 17 (1963) 626–637.

[13] J.C. Mailen, O.K. Talent, Solvent cleanup and degradation: A survey and recent ORNL results, Proceedings from ANS International Topical Meeting, Jackson Hole, Wyoming 1 (1984) 431–450.

[14] K.H. Eiben, H. Evers, P. Schween, H. Tatzel, Improved Solvent Treatment Reduces Amount of Waste in the PUREX-process, The Fourth International Confrence on Nuclear Fuel Reprocessing and Waste Management, RECOD'94, Volume-III, 1994.

[15] C. Ginisty, B. Guillaume, Solvent distillation for PUREX reprocessing plant, Sep. Sci. Technol. 25(13–15) (1990) 1941–1952.

[16] F. Sicilio, T.H. Goodgame, B. Wilkins, Jr., Purification of irradiated tributyl phosphate in kerosene type diluent by distillation, Nucl. Sci. Eng. 9 (1961) 455; also Engineering Experiment Station Georgia Institute of Technology, Final report on subcontract 1374 with ORNL, 1960.

[17] F. Drain, J.P. Moulin, D. Hugelmann, P. Lukas, Advance Solvent Management in Reprocessing: Five Years of Industrial Experience, ISEC'96 1996, 1789.

[18] B. Ya Zilberman, M.N. Makarychev-Mikhailov, V.F. Saprykin, L.B. Shpunt, S.V. Sakulin, Yu. N. Dulepov, V.V. Glushko, E. N. Semenov, N.A. Mikhailova, V.G. Balakhonov, M.E. Romanov, G.F. Egorov, O.P. Afanas'ev, V.I. Volk, Regeneration of spent TBP-diluent by steam distillation, Radiochemistry 44 (2002) 274–281.

[19] H.J. Clark, G.S. Nichols, Purification of Radioactive Solvent with Flash Vaporizer, USAEC Report DP-849, Savannah River Laboratory, 1965.

[20] P.R. Auchapt, R.R. Sautray, B.R. Girard, Solvent Purification Using a Current of Water Vapor, ORNL-tr-244, Translation of CEA-R 2404, Plutonium Production Centre at Marcoule, 1964.

[21] A.L. Olson, C.W. McCray, Solvent Regeneration Development at Idaho Chemical Processing Plant, ISEC'86, 1986, pp. 143–147.

[22] O.K. Talent, J.C. Mailen, K.D. Pannell, Solvent Cleanup Using Base Treated Silica Gel Solid Adsorbent, UD-DOE, Report, ORNL/RN-8948, 1984.

[23] J.C. Mailen, O.K. Talent, Cleanup of Savannah River Plant solvent using solid adsorbents, ORNL/TM-9256, Oak Ridge National Laboratory, Oak Ridge, TN, 1985.

[24] J.C. Mailen, Secondary Solvent Cleanup Using Activated Alumina: Laboratory, Development, CONF-871101-2, DE87-010603, 1987.

[25] E. Dermibas, M. Kobya, E. Senturk, T. Ozkan, Adsorption kinetics for the removal of Cr (VI) from aqueous solutions on the activated carbon prepared from agricultural wastes, J. Water 30(4) (2004) 533–539.

[26] A.E. Okoronkwo, S. Anwasi, Biosorption modeling of copper and zinc adsorption from aqueous solution by tithonia diverifolia, CSN Conference Proceedings, Chemical Society of Nigeria Deltachem (2008) 92–102.

[27] W.J. Weber, J.C. Morris, Kinetics of adsorption on carbon from solution, J. Sanitary Eng. Div. Proceed. Am. Soc. Civil Eng. 89 (1963) 31–59.

[28] J.D. Seader, Ernest J. Henley, D. Keith Roper, Separation Process Principles, 3rd ed., John Wiley & Sons, New York, NY, 2010.

[29] S. Lagergren, About the theory of so-called adsorption of solution substances, Kunglia srenska vertens Ka psakademiens, Handlinger 24 (1898) 147–156.

[30] Y.S. Ho, G. McKay, A two stage batch sorption optimized design for dye removal to minimize contact time, Trans. Inst. Chem. Eng. 76 (1998) 313–318.

[31] N.K. Pandey, P. Velavendan, R. Geetha, M.K. Ahmed, S.B. Koganti, Adsorption kinetics and breakthrough behaviour of tri-*n*-butyl phosphate on Amberlite XAD-4 Rresin, J. Nucl. Sci. Technol. 35(5) (1998) 370–378.

[32] I. Langmuir, The constitution and fundamental properties of solids and liquids part-I, J. Am. Chem. Soc. 38 (1916) 2221–2295.

[33] H.M.F. Freundlich, Over the adsorption in solution, J. Phys. Chem. 57 (1906) 385–470.

[34] D.M. Ruthven, Principles of Adsorption and Adsorption Processes, Wiley, New York, NY, 1984.

[35] F. Alexander, V.J.P. Poots, G. McKay, Adsorpotion kinetics and diffusional mass transfer processes during color removal from effluent using silica, Ind. Eng. Chem. Process Des. Dev. 17(4) (1978) 406–410.

Appendix A

The mass flow rate of solute through external film is proportional to the concentration difference between bulk phase DBP concentration (C) and DBP concentration at the particle surface C_s (R_p, t)

$$-\frac{\partial C}{\partial t} = \frac{3M_p k_f}{VR\rho_p}(C - C_s) \tag{A1}$$

The mass balance of DBP within a spherical particle is given as:

$$\varepsilon_p \frac{\partial C_r}{\partial t} + \rho_p \frac{\partial q_r}{\partial t} = D_e \frac{1}{r^2}\frac{\partial}{\partial r}\left(r^2 \frac{\partial C_r}{\partial r}\right) \tag{A2}$$

The Langmuir isotherm $\left(q_r = \frac{q_m K_L C_r}{1+K_L C_r}\right)$ can be used for the correlating of C_r and q_r. Then Eq. (A2) becomes

$$\frac{\partial C_r}{\partial t} = \frac{D_e}{\varepsilon_p + (\rho_p K_L q_m)/(1+K_L C_r)^2}\frac{1}{r^2}\frac{\partial}{\partial r}\left(r^2 \frac{\partial C_r}{\partial r}\right) \tag{A3}$$

The initial and boundary conditions can be written as:

$$t = 0 : C = C_0, Cr = 0 \tag{A4}$$

$$r = 0 : \left(\frac{\partial C_r}{\partial r}\right)_{r=0} = 0 \tag{A5}$$

$$r = R : k_f(C - C_S) = D_e\left(\frac{\partial C_r}{\partial r}\right)_{r=R} \tag{A6}$$

Eqs. (A1 and A3) can be written into dimensionless form as:

$$-\frac{\partial X}{\partial \theta} = Bi\frac{3M_p}{V\rho_p}(X - X_S) \tag{A7}$$

$$\begin{aligned}\frac{\partial X}{\partial \theta} &= \frac{1}{\varepsilon + (\rho_p K_L q_m)/(1+K_L C_0 X_r)^2} \\ &\quad \times \left(\frac{2}{X}\frac{X_r}{\partial X} + \frac{\partial^2 X_r}{\partial x^2}\right) \\ &= a_r \frac{1}{x^2}\frac{\partial}{\partial x}\left(x^2 \frac{X_r}{\partial x}\right)\end{aligned} \tag{A8}$$

and the initial and boundary conditions are:

$$\theta = 0 : X = 1, X_r = 0 \tag{A9}$$

$$x = 0 : \left(\frac{\partial X_r}{\partial x}\right)_{x=0} = 0 \tag{A10}$$

$$x = 1 : \left(\frac{\partial X_r}{\partial x}\right)_{x=1} = Bi(X - X_S) \tag{A11}$$

The dimensionless parameters are defined as:

$$\begin{aligned}&X = \frac{C}{C_0}, \quad X_r = \frac{C_r}{C_0}, \quad x = \frac{r}{R}, \quad \theta = \frac{tD_e}{R^2}, \\ &\text{and } \ Bi = \frac{k_f R}{D_e}\end{aligned} \tag{A12}$$

For solving set of partial differential Eqs. (A7) and (A8) they are changed to coupled ordinary differential equations by finite difference methods as follows:

$$\frac{dX_i}{d\theta} = a(i)\left[\frac{X_{i+1} - 2X_i + X_{i-1}}{(\Delta x)^2} + \frac{X_{i+1} - X_{i-1}}{x_i \Delta x}\right] \tag{A13}$$

Applying the boundary conditions (A10) and (A11), Eq. (A12) becomes at the center of the particle, $i = 1$,

$$\frac{dX_i}{d\theta} = a(1)\left[\frac{2(X_2 - X_1)}{(\Delta x)^2}\right]_{[since, at x=0, X_2 = X_0]} \tag{A14}$$

at the surface of the particle, $i = 1$,

$$\frac{dX_N}{d\theta} = a(N)\left[\frac{2X_{N-1} + 2\Delta x Bi(X - X_N) - 2X_N}{(\Delta x)^2} + Bi(X - X_N)\right] \tag{A15}$$

The total $N+1$ coupled ordinary differential equations for X, X_1, X_2, … are to be solved numerically in order to obtain concentration profiles.